Experimental Study of Electromagnetic Matrix Elements in ^{92}Mo†

S. Cochavi, J. M. McDonald, and D. B. Fossan
State University of New York, Stony Brook, New York 11790

(Received 6 November 1970)

The magnetic moment of the 2761-keV 8^+ state in ^{92}Mo has been measured as $\mu = (11.2 \pm 0.6)\mu_N$ ($g = 1.40 \pm 0.07$) using the ^{90}Zr$(\alpha, 2n)^{92}$Mo reaction and a time-differential technique. This result, which is consistent with a $|(1g_{9/2})^2, 8^+\rangle$ wave function, gives evidence for an enhanced g_I. The measurement also yielded a mean lifetime for the 8^+ state of $\tau = 275 \pm 10$ nsec. The lifetimes of the 2527-keV 5^- and 2613-keV 6^+ states were measured by p-γ and γ-γ delayed-coincidence methods, respectively. A mean life of $\tau = 2.24 \pm 0.06$ nsec was obtained for the 5^- state and the mean life of the 6^+ state was found to be $\tau = 2.22 \pm 0.07$ nsec. The observed $B(E2: 8^+ \rightarrow 6^+)$ and $B(E2: 6^+ \rightarrow 4^+)$ are consistent with $(1g_{9/2})^2$ proton configurations for the 4^+, 6^+, and 8^+ states. The lifetimes of the 6^+ and 5^- states imply that the $6^+ \rightarrow 5^-$ and $5^- \rightarrow 4^+$ $E1$ transitions in ^{92}Mo are hindered relative to the Weisskopf estimates by 2×10^4 and 7×10^4, respectively. These results are consistent with pure proton configurations of $(1g_{9/2})^2$ for the 4^+ and 6^+ states and $(2p_{1/2}, 1g_{9/2})$ for the 5^- state.

I. INTRODUCTION

The ^{92}Mo nucleus has been the subject of a considerable number of theoretical and experimental studies[1-6] in recent years. According to jj-coupling shell-model theory, protons in the region $38 < Z < 50$ are either in the $2p_{1/2}$ or $1g_{9/2}$ orbits. Thus, low-lying levels of the ^{92}Mo nucleus with the closed shell of 50 neutrons should manifest the $(1g_{9/2})^4$, $(1g_{9/2})^2(2p_{1/2})^2$, or $(1g_{9/2})^3(2p_{1/2})$ proton configurations. According to Vervier[1] and Auerbach and Talmi[2] the low-lying even-parity states of ^{92}Mo are due to admixtures of the $(2p_{1/2})^2(1g_{9/2})^2$ and $(1g_{9/2})^4$ proton configurations, while the negative-parity states have the $(2p_{1/2})(1g_{9/2})^3$ configuration. The 0_1^+ ground state, the 2_1^+ (1509-keV), 4_1^+ (2283-keV), 6_1^+ (2613-keV), and 8_1^+ (2761-keV) states are expected to be mixtures of $[(2p_{1/2})^2, 0^+][(1g_{9/2})^2, J]$ and $[(1g_{9/2})^4(v=2), J]$ configurations, and the 5^- (2527-keV) state should arise from the $[2p_{1/2}][(1g_{9/2})^3(v=1), \frac{9}{2}^+]$ configuration. The latter configuration is also expected to give rise to a 4^- state which has been predicted by Vervier[1] to be at 3.10 MeV, and by Auerbach and Talmi[2] to be at 2.95 MeV.

The 0_1^+, 2_1^+, 4_1^+, 6_1^+, and 8_1^+ levels in ^{92}Mo have been used for the calculation[1-3] of the effective proton-proton interaction in the $1g_{9/2}$ orbit. This effective interaction has been applied to a theoretical study of low-lying levels of nuclei in the mass-90 region with $40 \leq Z \leq 50$, $50 \leq N \leq 56$. Therefore, a measure of the purity of the $1g_{9/2}$ description is important.

The purpose of the present experiment is to check the simple configurations suggested for the structure of these states by experimentally determining electromagnetic matrix elements involving their wave functions. The low-lying states in ^{92}Mo are shown in Fig. 1. This study includes measurements of the magnetic moment of the 2.761-MeV 8^+ state and the electromagnetic transition prob-

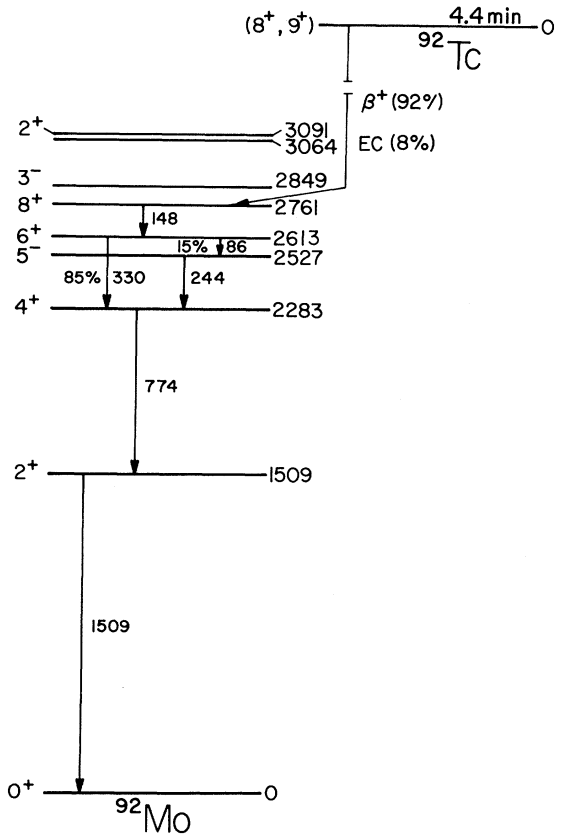

FIG. 1. Low-lying states in ^{92}Mo. The level scheme and spin-parity parameters are consistent with this work and that of Ref. 6.

abilities $B(E2:6^+\rightarrow 4^+)$, $B(E1:6^+\rightarrow 5^-)$, and $B(E1:5^-\rightarrow 4^+)$. In the suggested model the g factor for a $(1g_{9/2})^2$ 8^+ state is equal to the g factor for a single-proton $1g_{9/2}$ state; the latter can be deduced from the precise measurement[7] of the magnetic moment of the ^{93}Nb $\frac{9}{2}^+$ ground state. Thus, the experimental 8^+ g factor can be easily interpreted as a check on the simple $(1g_{9/2})^2$ wave function. The $E1$ electromagnetic transitions between the positive-parity states and the negative-parity states are sensitive to the purity of their wave functions because an $E1$ transition is forbidden between $2p_{1/2}$ and $1g_{9/2}$ shells. The $6^+\rightarrow 4^+$ $E2$-transition strength can be calculated in terms of $(1g_{9/2})^2$ wave functions and a $1g_{9/2}$ proton effective charge.

II. EXPERIMENTAL METHOD

A. Lifetime Measurement of the 2527-keV 5_1^- State

The lifetime of the 2527-keV 5_1^- state in ^{92}Mo was measured by a particle-γ delayed-coincidence technique using the ^{92}Mo$(p,p'\gamma)$ reaction. An excitation study of the ^{92}Mo$(p,p'\gamma)$ reaction was made between 6.0–9.0 MeV with a Ge(Li) γ detector at 90° and a annular particle detector at 180°. The optimum energy chosen for the lifetime measurement of the 5_1^- state was the analog resonance[6] at $E_p = 7.60$ MeV. The target was a self-supporting metal foil of 0.56-mg/cm^2 thickness enriched at 98% in ^{92}Mo.

The proton spectrum of the ^{92}Mo(p,p') reaction obtained at 7.60-MeV proton energy is shown in Fig. 2. Large proton groups corresponding to the 2_1^+, 4_1^+, and 5_1^- levels in ^{92}Mo are seen, while no observable groups exist for the 6_1^+, or the 8_1^+ levels. The 5_1^- proton group was used in the lifetime

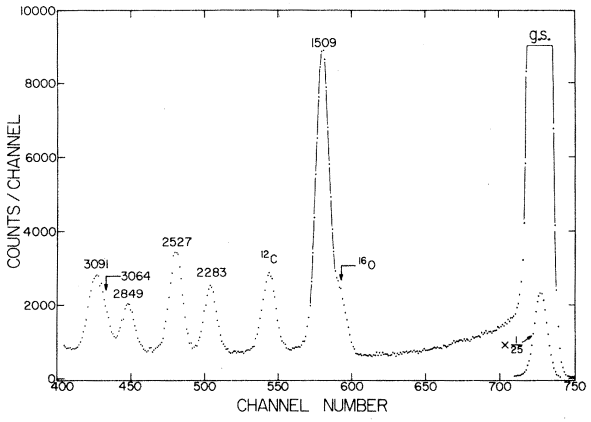

FIG. 2. Proton spectrum from the reaction ^{92}Mo(p,p'). The spectrum was taken at the analog resonance $E_p = 7.60$ MeV. The proton detector, an annular surface-barrier dectector, was placed at 180°. The proton groups are labeled by the energies of the final states.

measurement of the 5_1^- state while the 2_1^+ group was used to obtain the prompt-resolution function. Figure 3(b) shows a γ-ray singles spectrum of the ^{92}Mo$(p,p'\gamma)$ reaction observed at 90° with respect to the beam direction, at 7.60-MeV proton energy. It should be noted that because of the high (p,n) threshold, $Q_{\text{eff}} = -9.08$ MeV,[8] the γ singles spectrum does not include γ rays from the ^{92}Mo$(p,n\gamma)$ reaction. This γ spectrum shows a large 244-keV γ-ray yield which corresponds to the $5_1^-\rightarrow 4_1^+$ transition, while γ rays from the 6_1^+ and 8_1^+ states were not observed. The 244-keV $5_1^-\rightarrow 4_1^+$ γ transition was used for the lifetime measurement of the 5_1^- state. The γ rays observed at 480 and 537 keV have been previously identified[6] with transitions in ^{92}Mo, and γ rays at 304 and 365 keV are most likely from transitions between excited states at higher energies in ^{92}Mo.

The lifetime of the 5_1^- state was measured by a p-γ delayed-coincidence technique.[9] The lifetime result was obtained from the slope of the distribution of time delays between formation and decay of the state. The time of formation was determined by the detection of the 5_1^- proton group from the ^{92}Mo(p,p') reaction with a solid-state detector, while the time of decay was marked by the 244-keV $(5_1^-\rightarrow 4_1^+)$ γ ray detected in a NaI scintillator. The time-delay pulses were produced in a fast time-to-amplitude converter (TAC) in the usual fast-slow coincidence arangement. Time calibration of the TAC was made with air-dieletric delay lines.

An annular silicon detector of 1000-μ thickness and 100-mm^2 area was positioned at 180° to the beam direction. By means of an inductive pickoff, fast pulses for timing purposes were obtained from the protons; the normal energy pulses used for the slow-coincidence conditions were not effected by the pickoff circuit. The γ rays were detected by a $1\frac{1}{2}$-in.$\times 1\frac{1}{2}$-in. NaI scintillator coupled to an RCA 8575 phototube; its axis was placed at 90° to the beam direction. The fast-timing pulses were taken from the anode while the energy pulses were taken from a dynode farther up the phototube chain.

Figure 4 shows a schematic diagram of the experimental electronics. Slow-coincidence requirements were used in conjunction with the fast timing to isolate the states of interest and to minimize time jitter. For the NaI scintillator, the photopeak of the 244-keV γ ray was accepted in the pulse-height window of the single-channel analyzer (SCA) 1. This pulse-height window also accepted Compton events of the 1509-keV γ ray $(2_1^+\rightarrow 0_1^+)$ which were used for a measurement of the prompt-resolution function. The output of the proton amplifier (AMP 2) was fed into SCA 2 and SCA 3. SCA 2

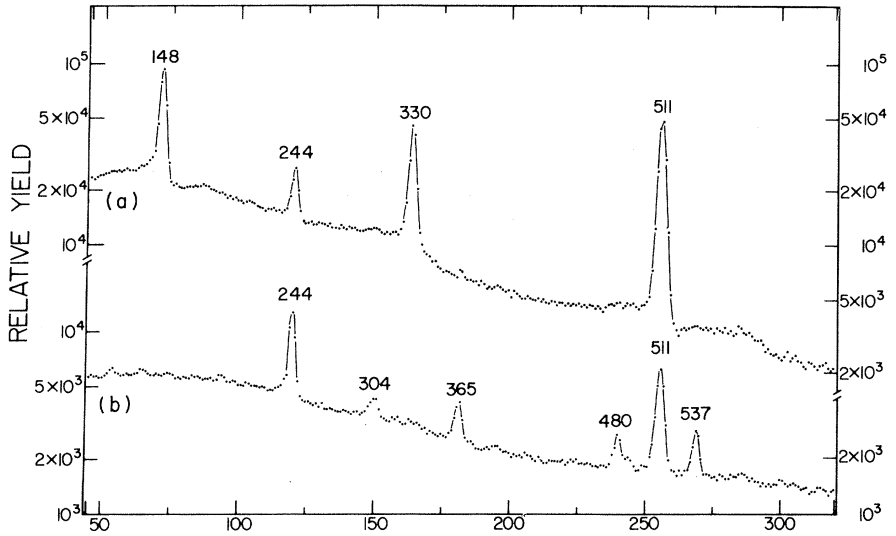

FIG. 3. Ge(Li) γ-ray spectra from γ transitions in ^{92}Mo. (a) γ-ray singles from 100 to 635 keV following the 4.4-min decay of ^{92}Tc. (b) γ-ray spectrum for the reaction ^{92}Mo-$(p,p'\gamma)$ measured at 7.60-MeV bombarding energy and at 90° to the beam direction.

accepted only the 2_1^+ proton group in its pulse-height window and SCA 3 the 5_1^- proton group. The outputs of SCA 2 and 3 were used to route the corresponding time-delay spectra into the different halves of a multichannel analyzer. Since the lifetime of the 2_1^+ state is known[10] to be short relative to the time resolution of this system, the time-delay spectrum associated with the 2_1^+ proton group and the 1509-keV γ rays represents the prompt-resolution function. Thus, the 5_1^- time-delay spectrum and the prompt-resolution function were measured simultaneously under identical conditions.

The filled circles in Fig. 5 show the time-delay spectrum for the 5_1^- proton group and the 244-keV γ ray. From several least-squares fits to different portions of the logarithmic slope, the extracted mean lifetime of the 2527-keV 5_1^- state is $\tau = 2.24 \pm 0.06$ nsec. The open circles in Fig. 5, which represent the prompt-resolution function, show the time spectrum for the 1509-keV 2_1^+ proton group and the same γ window.

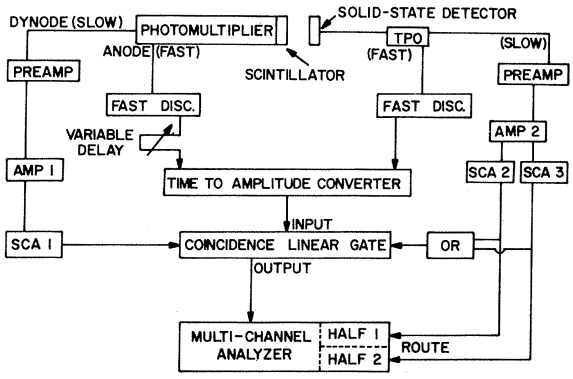

FIG. 4. A schematic diagram of the experimental electronics for the p-γ delayed-coincidence technique.

B. Lifetime Measurement of the 2613-keV 6_1^+ State

The 4.4-min ^{92}Tc isomeric β activity was used for the lifetime measurement of the 2613-keV ^{92}Mo 6_1^+ state. This activity was produced by bombarding a 0.57-mg/cm^2-thick ^{92}Mo foil with 12-MeV protons; Fig. 3(a) shows the γ-ray singles spectrum from 100 to 635 keV. Four prominent peaks were observed: the 148-keV $8_1^+ \rightarrow 6_1^+$ γ transition, the 244-keV $5_1^- \rightarrow 4_1^+$ γ transition following the 15% $6_1^+ \rightarrow 5_1^-$ branch, the 330-keV $6_1^+ \rightarrow 4_1^+$ γ transition, and the 511-keV γ ray from positron annihilation. The 148- and the 330-keV γ rays were used for the lifetime measurement of the 2613-keV 6_1^+ state.

The 6_1^+ lifetime was measured by a γ-γ delayed-coincidence technique. The lifetime result was obtained from a logarithmic slope of the distribution of the time delays between formation and decay of the state. The time of formation was determined by the detection of the 148-keV γ ray, while the time of decay was marked by the 330-keV γ ray. Two $1\frac{1}{2}$-in.$\times 1\frac{1}{2}$-in. NaI scintillators were used to detect the γ rays. Time-delay pulses were produced in a TAC from the fast signals provided at the anodes of the photomultiplier tubes. Appropriate dynode-pulse windows for the 148- and 330-keV photopeaks were required in the slow coincidence to isolate the 6_1^+ state and to optimize the time resolution. The use of the 330-keV γ-ray photopeak for the lifetime measurement of the 6_1^+ state essentially eliminated any contributions from the lifetime of the 5_1^- state which is fed by the 15% branch. The γ-γ timing measurement was carried out in cycles using a beam shutter: first, the target was activated with the beam on for 1 min;

then with the beam off, the short-lived activities were allowed to decay for a 0.5-min delay; and finally the timing data were taken for 3.5 min.

The resulting time-delay spectrum for the 2613-keV 6_1^+ state in ^{92}Mo is shown in Fig. 6 by the filled circles and the solid line. From several least-squares fits to different portions of the logarithmic slope, the extracted mean lifetime of the 6_1^+ state in ^{92}Mo is $\tau = 2.22 \pm 0.07$ nsec. The open circles and the dashed line represent an upper limit of the resolution function; this limit was measured with the 14.6-h ^{90}Nb source under similar experimental conditions yielding an upper limit of $\tau \leq 0.36$ nsec for the mean lifetime of the 6_1^+ state in ^{90}Zr.

C. Excitation Study of the γ-Ray Spectra from ^{90}Zr + α

An α beam from the Stony Brook tandem accelerator was used to study γ-ray yields from ^{90}Zr + α as a function of energy to investigate the usefulness of the ^{90}Zr$(\alpha, 2n)^{92}$Mo reaction. A self-supporting 3-mg/cm^2 ^{90}Zr foil enriched to 98% in ^{90}Zr was used as a target. The γ detector, a 30-cc Ge(Li) crystal, was placed at 90° to the beam direction. The detector energy resolution was approximately 3.5 keV for the 1332-keV ^{60}Co γ ray.

Figure 7 shows γ spectra from ^{90}Zr + α at bombarding energies from 20 through 24 MeV in 1-MeV intervals. Strong γ transitions identified with the known low-lying levels in ^{92}Mo and ^{93}Mo are observed, while no prominent γ rays in ^{90}Zr, ^{92}Zr, ^{92}Nb, or ^{92}Nb are seen; this indicates that at these bombarding energies the dominant reactions are ^{90}Zr$(\alpha, n)^{93}$Mo and ^{90}Zr$(\alpha, 2n)^{92}$Mo. In this excitation study, there are two groups of prominent γ rays. The yield of group 1 increases while that of group 2 decreases as a function of increasing α energy in the region $E_\alpha = 20$–24 MeV. Group 1 is identified[11] with the ^{90}Zr$(\alpha, 2n)^{92}$Mo reaction; the γ transitions from this reaction are marked by a downward arrow in Fig. 7 and are listed in Table I. Group 2 contains four γ rays identified with known[12,13] γ transitions in ^{93}Mo which are populated via the ^{90}Zr$(\alpha, n)^{93}$Mo reaction; they are marked by an upward arrow in Fig. 7 and are listed in Table II together with the other γ rays in the group which are unidentified but which probably result from the same reaction.

As shown in Fig. 7 there are five prominent peaks from ^{92}Mo at $E_\alpha = 24$ MeV in addition to the 511-keV annihilation γ rays: 148, 244, 330, 774, and 1509 keV. The 148-keV $8_1^+ \rightarrow 6_1^+$ γ transition has a sufficient yield to be used for the magnetic-moment measurement of the 8_1^+ state in ^{92}Mo. A

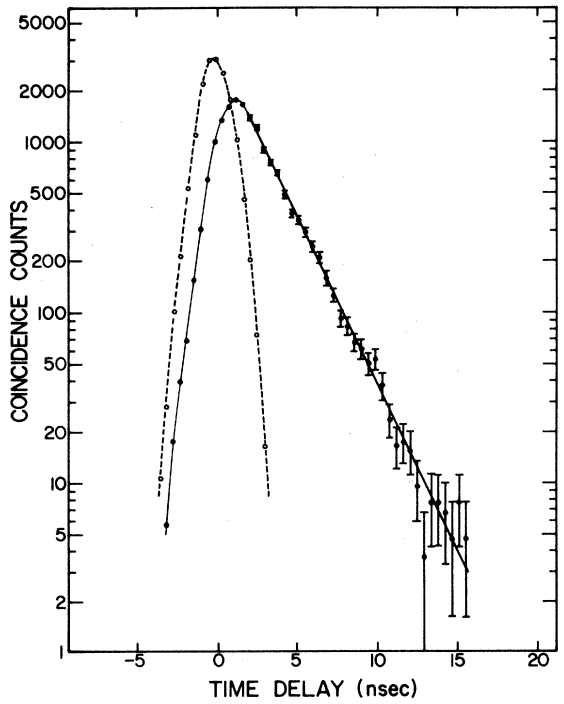

FIG. 5. The experimental decay curve for the 2527-keV 5_1^- state in ^{92}Mo. The decay curve for the 5_1^- state is shown with filled circles and the solid line. The right slope of the decay curve corresponds to a mean life $\tau = 2.24 \pm 0.06$ nsec. The open circles represent the prompt-resolution function.

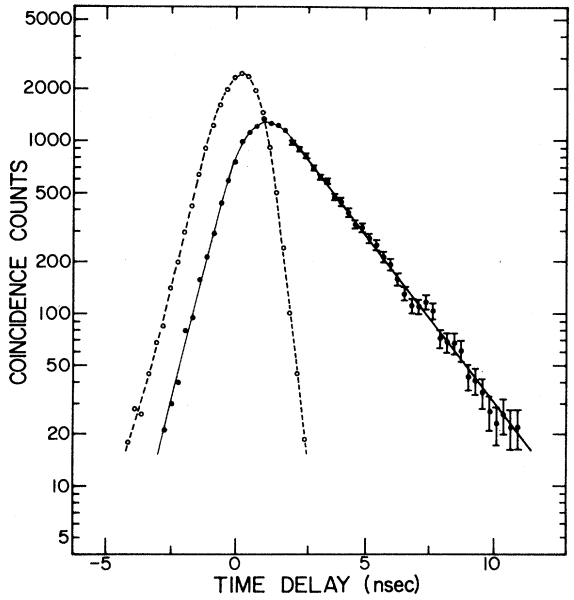

FIG. 6. The experimental decay curve for the 2613-keV 6_1^+ state in ^{92}Mo. The decay curve for the 6_1^+ state is shown with the filled circles and solid line. The right slope of the decay curve corresponds to a mean life $\tau = 2.22 \pm 0.07$ nsec. The open circles represent the prompt-resolution function.

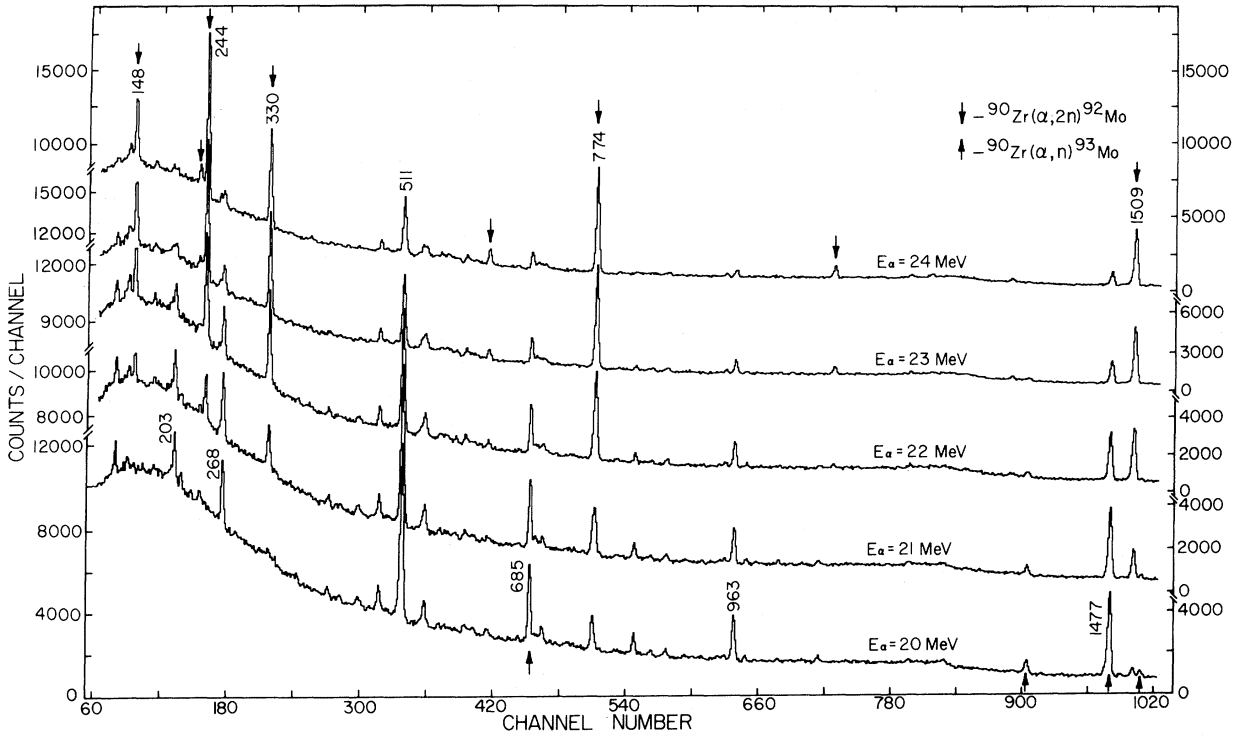

FIG. 7. γ-ray spectra from $^{90}Zr+\alpha$ at bombarding energies E = 20, 21, 22, 23, and 24 MeV. The Ge(Li) detector was placed at 90° to the beam direction. The γ energies in keV units are written for the prominent peaks in the upper and lower spectra.

comparison of this spectrum with the γ rays observed in the decay of the 4.4-min ^{92}Tc shown in Fig. 3(a) indicates that the 5^- state in ^{92}Mo is strongly populated by the $^{90}Zr(\alpha,2n)^{92}Mo$ reaction. No prominent γ transition in Fig. 7 can be associated with the corresponding 4^- state expected[1,2] at ~3 MeV.

D. Magnetic Moment of the 2761-keV 8_1^+ State

The magnetic moment of the 8_1^+ state in ^{92}Mo was measured by a time-differential perturbed-angular-correlation technique.[14] The time-dependent correlation function $W(\theta,t)$ for the detection of a γ ray emitted from a nucleus, aligned with respect to the beam direction, in a magnetic field B perpendicular to the plane defined by the beam and

TABLE I. γ rays from $^{90}Zr+\alpha$ at E_α = 20–24 MeV which are increasing with E_α.

E_γ (keV)	Nucleus	$J^\pi_i \rightarrow J^\pi_f$	E_i (keV)	E_f (keV)
148	^{92}Mo	$8^+ \rightarrow 6^+$	2761	2613
235	^{92}Mo	$(11^-) \rightarrow (9^-)$	4486 [a]	4251
244	^{92}Mo	$5^- \rightarrow 4^+$	2427	2283
330	^{92}Mo	$6^+ \rightarrow 4^+$	2527	2283
627	^{92}Mo	$(9^-) \rightarrow (7^-)$	4251 [a]	3624
774	^{92}Mo	$4^+ \rightarrow 2^+$	2283	1509
1097	^{92}Mo	$(7^-) \rightarrow 5^-$	3624 [a]	2527
1509	^{92}Mo	$2^+ \rightarrow 0^+$	1509	0

[a] Taken from Ref. 11.

TABLE II. γ rays from $^{90}Zr+\alpha$ at E_α = 20–24 MeV which are decreasing with E_α.

E_γ (keV)	Nucleus	$J^\pi_i \rightarrow J^\pi_f$	E_i (keV)	E_f (keV)
124				
203				
268				
480				
538				
685	^{93}Mo	$\frac{13}{2}^+ \rightarrow \frac{9}{2}^+$	2162 [a]	1477
702				
827				
964				
1364	^{93}Mo	$\frac{7}{2}^+ \rightarrow \frac{5}{2}^+$	1364 [a]	0
1477	^{93}Mo	$\frac{9}{2}^+ \rightarrow \frac{5}{2}^+$	1477 [a]	0
1522	^{93}Mo	$(\frac{7}{2}^+) \rightarrow \frac{5}{2}^+$	1522 [a]	0

[a] Taken from Refs. 12 and 13.

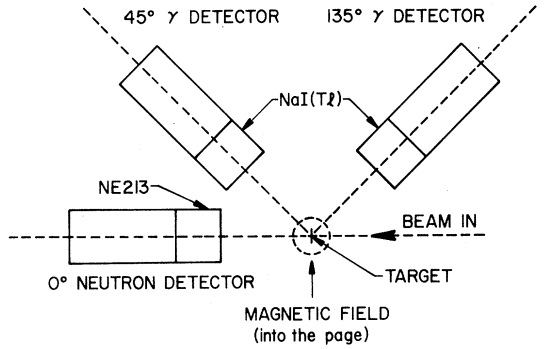

FIG. 8. A sketch of the experimental arrangement for the magnetic-moment measurement of the 8_1^+ state in ^{92}Mo.

the direction of emission of the γ ray is

$$W(\theta,t)=\sum_{k\ \text{even}} A_k P_k[\cos(\theta\pm\omega_L t)]e^{-t/\tau}, \quad (1)$$

where ω_L is the Larmor precession frequency, $P_k(\cos\theta)$ is a Legendre polynomial of order k, and τ is the mean life of the state under consideration. The Larmor frequency depends on the g factor and the magnetic field B as $\omega_L = g\mu_N B/\hbar$ where μ_N is the nuclear magneton.

In the present case, the transition $8_1^+ \rightarrow 6_1^+$ involves $E2$ radiation, and terms in Eq. (1) up to $k=4$ are expected. A convenient way of extracting ω_L from the time-differential data is to generate the function

$$R(t)=[Y(135,t)-Y(45,t)]/[Y(135,t)+Y(45,t)], \quad (2)$$

where $Y(\theta,t)$ represents the yield as a function of the angle θ and delay time t. For the case where $A_4 \ll 1$ as was found for this measurement, $R(t)$ has the form $R(t)=[3A_2/(4+A_2)]\sin(2\omega_L t)$. A value for ω_L can be obtained by fitting the experimental $R(t)$ to the function $\sin(2\omega_L t)$. The g factor can then be directly determined from the above expression for the Larmor frequency.

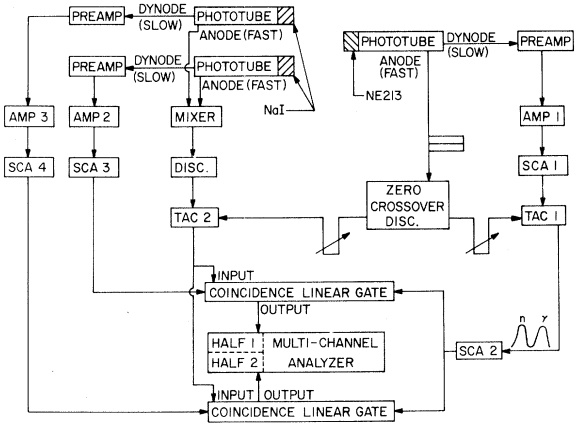

FIG. 9. A schematic diagram of the experimental electronics of the n-γ time-differential perturbed-angular-correlation technique.

A sketch which shows the general experimental arrangement used in the magnetic-moment measurement of the ^{92}Mo 8_1^+ state is shown in Fig. 8. The reaction ^{90}Zr$(\alpha,2n)^{92}$Mo was used to populate the 8_1^+ state at a bombarding energy of 24 MeV. The target was a 3-mg/cm^2 self-supporting ^{90}Zr foil. To minimize the background radiation, the beam collimator and beam stop were made of bismuth. A magnetic field of 3.8 ± 0.1 kG at the target spot was provided by an electromagnet. The magnetic field was measured with a gaussmeter and checked by a (p,p') time-differential measurement of the magnetic moment of the 197-keV $\frac{5}{2}^+$ state in ^{19}F. The γ detectors, $1\frac{1}{2}$-in.$\times 1\frac{1}{2}$-in. NaI crystals, were placed 8 cm from the target at 45 and 135° with respect to the beam direction. The target chamber was made of glass with thin walls which had minimal absorption for the 148-keV γ ray.

The neutron detector was a 2-in.$\times$2-in. NE213 liquid scintillator coupled to an RCA 8575 phototube. Its axis was placed at 0° to the beam direction and at 8 cm from the center of the target. A disk of lead, $\frac{1}{8}$ in. thick was placed in front of the

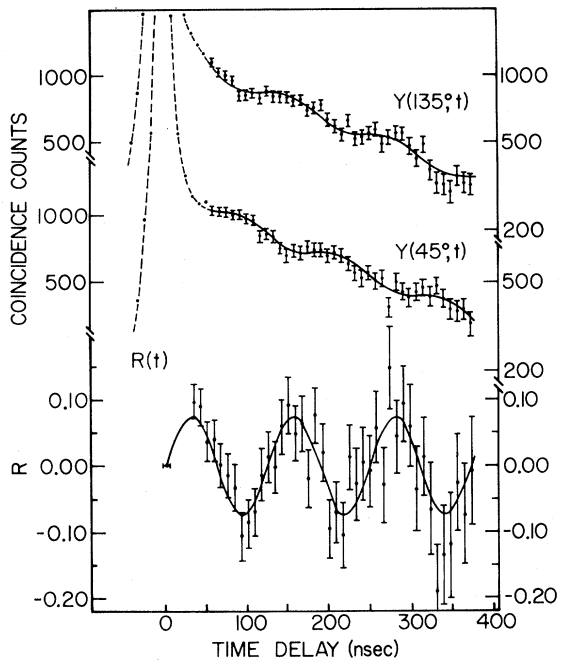

FIG. 10. The perturbed-time-delay curves $Y(135,t)$ and $Y(45,t)$, and the function $R(t)$ for the 2.761-MeV 8_1^+ state in ^{92}Mo. The solid curve shown for the $R(t)$ data is a least-squares fit of $\sin 2\omega_L t$. The solid curves drawn through the $Y(45,t)$ and $Y(135,t)$ data were generated theoretically with the amplitude and the frequency obtained from the least-squares fit of $R(t)$.

neutron detector to attenuate low-energy γ rays. Neutron-γ pulse-shape discrimination was used to select the neutrons.[15] The neutron-induced recoil-proton pulses exhibit a larger slow-decay component than the γ-produced Compton-electron pulses. These different pulse shapes were identified by measuring the time delay between the fast component observed at the anode and the bipolar cross-over of the corresponding integrated dynode signal. A measurement of this time difference for each pulse with a TAC allows the selection of only neutrons. The neutron-γ pulse-shape discriminator is shown in the right part of Fig. 9. The pulse-height region appropriate to neutrons from TAC 1 was selected by SCA 2.

In this measurement, pulses from the neutron detector corresponding to an energy between 0.5 and 3.5 MeV were used to start TAC 2 as shown in Fig. 9; the photopeak pulses for the 148-keV γ rays from the NaI detectors provided the stop signals. The resulting time-delay spectra for the 45 and the 135° γ detectors were collected in different halves of the multichannel analyzer. In this way the precession of the angular correlation could be observed simultaneously at both 45 and 135° with respect to the beam direction. The time resolution of the system was about 5-nsec full width at half maximum and the time calibration was made with air-dielectric trombone delay lines.

The results for several runs for a total of about 20 h with an α beam current of ~1 nA are shown in Fig. 10. The time spectra $Y(135,t)$ and $Y(45,t)$ are shown in the upper portion of the figure. Out-of-phase modulations in the two logarithmic time slopes can be seen which indicate the existence of a $P_2(\cos\theta)$ component in the time-dependent correlation function $W(\theta,t)$. Figure 11 shows the sum spectrum; no prominent perturbation that can be associated with $P_4(\cos\theta)$ is seen. This indicates that $|A_4| \ll 1$, and that the ratio $R(t)$ can be analyzed in terms of Eq. (2). The ratio $R(t)$ formed from the experimental data is shown in the lower part of Fig. 10. After consideration of beam-bending effects, $R(t=0)$ has been set equal to zero. A least-squares fit of the observed $R(t)$ to $\sin 2\omega_L t$ and a Fourier-transform analysis of the data result in a Larmor frequency of $\omega_L = (2.55 \pm 0.12) \times 10^7$ sec^{-1}. From this value of ω_L, the g factor for the 2761-keV 8_1^+ state in ^{92}Mo is $g = 1.40 \pm 0.07$, and the magnetic moment is $\mu = (11.2 \pm 0.6)\mu_N$. The curves shown in Fig. 10 represent the best fit to the data.

The amplitude obtained from the least-squares fit was 0.073. Taking into consideration the geometric attenuation coefficient $Q_2 = 0.96$ for a 148-keV γ ray, the resulting A_2 is 0.099 ± 0.010. This value of A_2 is less than that expected[16] from the $(\alpha, 2n)$ reaction. The calculated average recoil distance of the appropriate Mo ions in the ^{90}Zr target is less than 250 μg/cm^2; hence, with the ~3-mg/cm^2 Zr target more than 90% of the ^{92}Mo ions stop in the target. This suggests an attenuation of the alignment in the Zr metal. As shown in the lower part of Fig. 10, no significant attenuation is observed in A_2 over the time region 40–400 nsec.

The mean life obtained from fitting the total sum spectrum which is displayed in Fig. 11 is $\tau = 275 \pm 10$ nsec. The mean-life result is in agreement with the two previous measurements[11,17]; Löbner[17] used 4.4-min ^{92}Tc β^+ decay to populate this state and Jaklevic *et al.*[11] employed the pulse-beam technique using the ^{90}Zr $(\alpha, 2n)^{92}$Mo reaction.

III. DISCUSSION

The summary of the present experimental lifetime information obtained for states in ^{92}Mo is given in Table III; previous lifetime information is also included. In addition, the g factor of the 2.761-MeV 8_1^+ state in ^{92}Mo was measured to be $g = 1.40 \pm 0.07$. For comparison with the present experimental results, transition-probability calculations

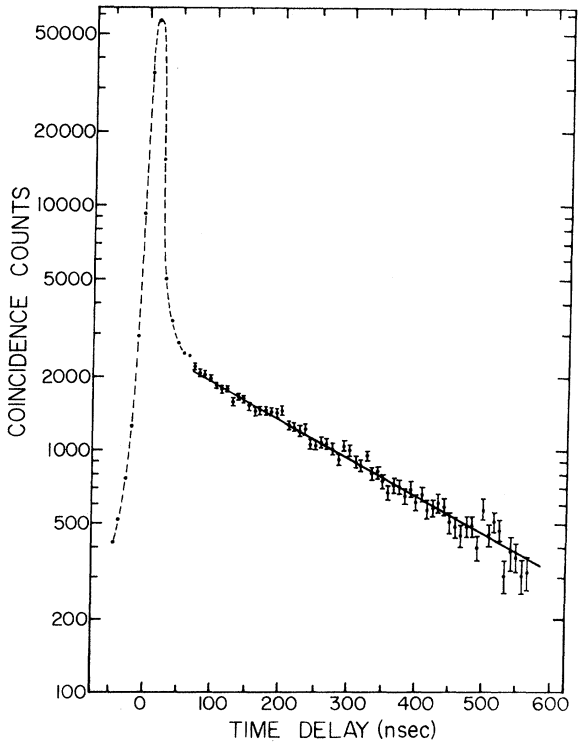

FIG. 11. Lifetime decay curve for the 2.761-MeV 8_1^+ state in ^{92}Mo. The decay curve for the 8_1^+ state was obtained from the total sum spectrum $[Y(135,t) + Y(45,t)]$. The right slope of the decay curve corresponds to a mean lifetime $\tau = 275 \pm 10$ nsec.

have been made using $(1g_{9/2})^2$ proton configurations for the 0_1^+, 2_1^+, 4_1^+, 6_1^+, and 8_1^+ levels. The $E1$ transitions involving the 5_1^- state are also considered. A g-factor calculation has been made in terms of the same configuration and the empirical g factor of a single $1g_{9/2}$ proton, which can be deduced from the experimental[7] g factor of ^{93}Nb ground state and its wave function as given by Sheline *et al.*[18] Additional admixtures in the 8_1^+ state have also been considered.

The mean lifetime of the 8_1^+ state in ^{92}Mo obtained from the magnetic-moment measurement is $\tau = 275 \pm 10$ nsec. This 8_1^+ state decays via an $E2$ transition to the 6_1^+ state. For this transition the theoretical total internal-conversion coefficient[19] is 0.29. Taking this into consideration the experimental $B(E2: 8_1^+ \rightarrow 6_1^+)$ equals $64.8 \pm 3.3\ e^2\,\mathrm{F}^4$ as listed in Table IV. The mean-lifetime result for the 6_1^+ state in ^{92}Mo is $\tau = 2.22 \pm 0.07$ nsec. This result, the 85% branching ratio to the 4_1^+ state, and the theoretical internal-conversion coefficient of 0.018 give an experimental $B(E2: 6_1^+ \rightarrow 4_1^+)$ of $156.9 \pm 7.8\ e^2\,\mathrm{F}^4$. The experimental $B(E2: 2_1^+ \rightarrow 0_1^+)$, also listed in Table IV for comparison purposes, has been taken from Ref. 10. Assuming the 0_1^+, 2_1^+, 4_1^+, 6_1^+, 8_1^+ multiplet to be a pure $(1g_{9/2})^2$ proton configuration, the theoretical reduced transition probabilities $B(E2)$ have been calculated. Only slight changes occur if an admixture of seniority-two $(1g_{9/2})^4$ and $(2p_{1/2})^2(1g_{9/2})^2$ configurations is used. Harmonic-oscillator wave functions were used for the radial integral; the oscillator parameter was deduced from a comparison of the experimental R_{rms} of ^{90}Zr obtained from electron scattering data[20] with that for particles filling the appropriate harmonic-oscillator shells. The resulting theoretical $B(E2)$'s are listed in column 5 of Table IV. The proton effective charge (e_π) is defined as the square root of the ratio $B(E2)_{\mathrm{exp}}/B(E2)_{\mathrm{th}}$; the e_π values are listed for the different $E2$ transitions in column 6. The e_π is used to account for the quadrupole polarization of the core. As shown in column 6, e_π is approximately the same for $8^+ \rightarrow 6^+$ and $6^+ \rightarrow 4^+$ $E2$ transitions; although the e_π for the $2^+ \rightarrow 0^+$ transition is slightly larger, it still agrees within the uncertainties with the other e_π values. This agreement of the e_π values for the three $E2$ transitions listed in Table IV is consistent with the assumption of the $|\pi(1g_{9/2})^2, J^+\rangle$ configurations for the 0_1^+, 2_1^+, 4_1^+, 6_1^+, 8_1^+ states in ^{92}Mo. The observed magnitude of e_π agrees with previous information for the $1g_{9/2}$ e_π in ^{92}Nb.[14] No calculations of the e_π in this mass region have been made. Any collective components,[21] which might be expected to admix most easily into the lower members of this group of states, would greatly increase the corresponding $B(E2)$ values relative to the above description; since the deduced e_π for the $2_1^+ \rightarrow 0_1^+$ is similar to that for the $8_1^+ \rightarrow 6_1^+$ and $6_1 \rightarrow 4_1$ transitions, such collective admixtures appear to be small.

The mean lifetime of the 5_1^- state was measured in this experiment to be $\tau = 2.24 \pm 0.06$ nsec. The 5_1^- state decays via an $E1$ γ transition to the 4_1^+ state; its lifetime is hindered with respect to single-particle estimates by a factor of $\sim 7 \times 10^4$. The $B(E1: 6_1^+ \rightarrow 5_1)$ strength, obtained from the lifetime of the 6_1^+ state and the 15% $(6_1^+ \rightarrow 5_1^-)$ branching ratio, is hindered by a factor of $\sim 2 \times 10^4$ relative to single-particle estimates. These large hindrances are consistent with the assumption that the 4_1^+ and 6_1^+ states are $(1g_{9/2})^2$ configurations and that the 5_1^- state is a $(2p_{1/2}, 1g_{9/2})$ configuration, because $E1$ transitions are not allowed between the $2p_{1/2}$ and the $1g_{9/2}$ orbits. These values of the $E1$ hindrance imply admixtures with amplitudes $< 7 \times 10^{-3}$; the most likely admixtures are the $2d_{3/2}$ configuration in the 6_1^+ and 4_1^+ state and the $1h_{11/2}$ configuration in the 5_1^- state. These results indicate very pure $(1g_{9/2})^2$ and $(2p_{1/2}, 1g_{9/2})$ proton configurations for the two unpaired particles of the corresponding 6_1^+, 4_1^+, and 5_1^- states.

The g factor of the 8_1^+ state in ^{92}Mo was measured to be $g = 1.40 \pm 0.07$. This value can be compared with the g factor calculated for a

TABLE III. Summary of lifetimes for states in ^{92}Mo.

E (keV)	J^π	τ (mean lifetime)
1509	2^+	0.89 ± 0.15 psec [a]
2527	5^-	2.24 ± 0.06 nsec [b]
2613	6^+	2.22 ± 0.07 nsec [b]
2761	8^+	277 ± 10 nsec [c]
		317 ± 43 nsec [d]
		275 ± 10 nsec [b]
4486	(11^-)	12.7 ± 0.7 nsec [d]

[a] Calculated from $B_{\mathrm{expt}}(E2: 0_1^+ \rightarrow 2_1^+)$ of Ref. 10.
[b] Present results.
[c] Taken from Ref. 11.
[d] Taken from Ref. 17.

TABLE IV. $E2$ transitions in ^{92}Mo.

E_i (keV)	$J^\pi_i \rightarrow J^\pi_f$	E_γ (keV)	$B(E2)\,e^2\,\mathrm{F}^4$ Expt.	$B(E2)\,e^2\,\mathrm{F}^4$ Theory [a]	e_π [b]
2761	$8^+ \rightarrow 6^+$	148	64.8 ± 3.8	15.07	2.07 ± 0.10
2613	$6^+ \rightarrow 4^+$	330	156.8 ± 7.8	37.64	2.04 ± 0.10
1509	$2^+ \rightarrow 0^+$	1509	234 ± 40 [c]	47.37	2.22 ± 0.38

[a] Theoretical calculations based on harmonic wave functions of $(1g_{9/2})^2$; the harmonic-oscillator parameter was deduced from the experimental R_{rms} of ^{90}Zr.
[b] $(e_\pi)^2 = B(E2)_{\mathrm{expt}}/B(E2)_{\mathrm{th}}$.
[c] Taken from Ref. 10.

$|\pi(1g_{9/2})^2, 8^+\rangle$ wave function. For shell-model states composed of two identical particles and for an additive single-particle magnetic-moment operator, the g factor for the two-particle state $g(|j^2, J^+\rangle)$ equals the g factor for the single-particle state $g(|j\rangle)$. The g factor for a state $|\pi(1g_{9/2})^2, 8^+\rangle$ is thus equal to the single-proton $g(|g_{9/2}\rangle)$. Since the g factor for the ^{91}Nb $\frac{9}{2}^+$ ground state has not been measured, the empirical $g(|1g_{9/2}\rangle)$ can instead be deduced from the known g factor and wave function of the ^{93}Nb $\frac{9}{2}^+$ ground state; only small corrections for seniority-three configurations involving $2d_{5/2}$ neutrons are necessary. The wave function for the ^{93}Nb ground state is given by Sheline *et al.*[18] as

$$|^{93}\text{Nb}, \tfrac{9}{2}^+\rangle = \sum b_i |[\nu(2d_{5/2})^2, J_i][\pi(1g_{9/2})], \tfrac{9}{2}^+\rangle , \quad (3)$$

where $b_0 = 0.94$, $b_2 = 0.33$, and $b_4 = 0.08$; the ^{93}Nb ground-state g factor has been measured[7] as $g(|^{93}\text{Nb}, \frac{9}{2}^+\rangle) = 1.3707$. By equating the g factor calculated from the wave function given in Eq. (3) with the ^{93}Nb experimental value, the $g(|1g_{9/2}\rangle)$ is obtained with only a very weak dependence on $g(|2d_{5/2}\rangle)$, which was taken as the measured[22] g factor of the ^{91}Zr $\frac{5}{2}^+$ ground state. The resulting empirical $g(|1g_{9/2}\rangle)$ equals 1.40, which is only slightly reduced from the free-nucleon value of 1.51. This value agrees perfectly with the experimental value for the ^{92}Mo 8^+ state of $g = 1.40 \pm 0.07$. This agreement shows that with respect to the magnetic-moment operator, the $|(1g_{9/2})^2, 8^+\rangle$ wave function describes well the 2.761-MeV state in ^{92}Mo. Of course, the magnetic-moment operator is not sensitive to whether these two particles are part of the seniority-two $(1g_{9/2})^4$ or $(2p_{1/2})^2(1g_{9/2})^2$ configurations.

On the basis of the uncertainties in the present experimental g factor, estimates can be made on the purity of the suggested wave function. The most likely shell-model admixture in the 8^+ state would involve the $1g_{7/2}$ shell. Assuming a wave function of $[a|(1g_{9/2})^2, 8^+\rangle + b|(1g_{9/2}, 1g_{7/2}), 8^+\rangle]$ and the free-nucleon $1g_{7/2}$ g factor of 0.49, the experimental uncertainties limit the admixture to $b^2 \leq 5\%$ on the basis of a calculation of the 8^+ g factor. This argument is based on the fact that the amplitudes a and b have the same phase, which is the case for a δ-function interaction and is expected for other reasonable interactions. Likewise, admixtures for deformed-rotational components with g factors of ~0.5 are limited to about 10% by the experimental uncertainties. These theoretical considerations of g-factor sensitivity for different admixtures along with the experimental uncertainties imply that the wave function of the 2.761-MeV 8^+ state of ^{92}Mo is a very pure $|(1g_{9/2})^2, 8^+\rangle$ configuration.

From the present experimental results and the information on the ^{93}Nb ground state, the $g(|1g_{9/2}\rangle)$ is fairly well established as 1.40. This value as compared with the free-nucleon value of 1.51 is somewhat larger than would be expected on the basis of core-polarization reductions of g_s.[23,24] An estimate of these effects for the ^{91}Nb $\frac{9}{2}^+$ ground state[24] gives a $g(|1g_{9/2}\rangle)$ of 1.32. Relative to this value, the larger experimental $g(|1g_{9/2}\rangle)$ gives evidence for an enhanced g_l of $\delta g_l \sim 0.09$ as has been observed[25] in ^{210}Po. The enhanced orbital magnetism is believed to be the result of meson-exchange effects.

In summary, the magnetic-moment measurement[26] of the 8_1^+ state in ^{92}Mo and the measured $E2$ strengths $8_1^+ \to 6_1^+$ and $6_1^+ \to 4_1^+$ are consistent with $|\pi(1g_{9/2})^2, J^+\rangle$ configurations for the corresponding 4_1^+, 6_1^+, 8_1^+ states in ^{92}Mo. In addition, the measured $B(E1 : 6_1^+ \to 5_1^-)$ and $B(E1 : 5_1^- \to 4_1^+)$ suggest a pure $(2p_{1/2}, 1g_{9/2})$ configuration for the 5_1^- state.

ACKNOWLEDGMENT

We are grateful to Dr. Jan Blomquist for helpful theoretical discussions.

---

†Work supported in part by the National Science Foundation.

[1]J. Vervier, Nucl. Phys. 75, 17 (1966).
[2]N. Auerbach and I. Talmi, Nucl. Phys. 64, 458 (1965).
[3]K. H. Bhatt and J. B. Ball, Nucl. Phys. 63, 286 (1965); J. B. Ball, J. B. McGrory, R. L. Auble, and K. H. Bhatt, Phys. Letters 29B, 182 (1969).
[4]J. K. Dickens, E. Eichler, R. J. Silva, and I. R. Williams, Phys. Letters 21, 657 (1966).
[5]E. J. Martens and A. M. Bernstein, Nucl. Phys. A117, 241 (1968).
[6]K. P. Lieb, T. Hausmann, and J. J. Kent, Phys. Rev. 182, 1341 (1969).
[7]I. Lingdren, Arkiv Fysik 29, 553 (1965).
[8]C. F. Moore, P. Richard, C. E. Watson, D. Robson, and J. D. Fox, Phys. Rev. 141, 1166 (1966).
[9]S. Cochavi, N. Cue, and D. B. Fossan, Phys. Rev. C 1, 1821 (1970).
[10]P. H. Stelson and L. Grodzins, Nucl. Data 1, 21 (1965).
[11]J. M. Jaklevic, C. M. Lederer, and J. M. Hollander, Phys. Letters 29B, 179 (1966).
[12]P. Alexander and G. Scharff-Goldhaber, Phys. Rev. 151, 964 (1966).
[13]C. M. Lederer, J. M. Hollander, and I. Perlman, *Table of Isotopes* (John Wiley & Sons, Inc., New York,

1967), 6th ed.
[14]H. Frauenfelder and R. M. Steffen, in *Alpha-, Beta- and Gamma-ray Spectroscopy*, edited by K. Siegbahn (North-Holland Publishing Company, Amsterdam, The Netherlands, 1965), Vol. 2, p. 1151ff.
[15]S. Cochavi and D. B. Fossan, Phys. Rev. C 3, 275 (1971).
[16]T. Yamazaki, T. Nomura, U. Katou, T. Inamura, A. Hashizume, and Y. Tendou, Phys. Rev. Letters 24, 317 (1970).
[17]K. E. Löbner, Nucl. Phys. 58, 49 (1964).
[18]R. K. Sheline, R. T. Jernigan, J. B. Ball, K. H. Bhatt, Y. E. Kim, and J. Vervier, Nucl. Phys. 61, 342 (1965).
[19]R. S. Hager and E. C. Seltzer, Nucl. Data A4, 1 (1968).
[20]J. Bellicard, P. Leconte, T. H. Curtis, R. A. Eisenstein, D. Madsen, and C. Bockelman, Nucl. Phys. A143, 213 (1970).
[21]S. Cochavi, D. B. Fossan, S. H. Henson, D. E. Alburger, and E. K. Warburton, Phys. Rev. C 2, 2241 (1970).
[22]E. Brun, J. Oeser, and H. H. Staub, Phys. Rev. 105, 1929 (1957).
[23]J. Blomquist, N. Freed, and H. O. Zetterstrom, Phys. Letters 18, 47 (1965).
[24]L. S. Kisslinger and R. A. Sorenson, Rev. Mod. Phys. 35, 853 (1963).
[25]T. Yamazaki, T. Nomura, S. Nagamiya, and T. Katou, Phys. Rev. Letters 25, 547 (1970).
[26]S. Cochari, J. M. McDonald, and D. B. Fossan, Phys. Letters 33B, 297 (1970).

PHYSICAL REVIEW C VOLUME 3, NUMBER 3 MARCH 1971

High-Resolution Study of Nb^{92} by (d, t) and $(d, t\gamma)$ Reactions*

T. S. Bhatia, W. W. Daehnick, and T. R. Canada
Nuclear Physics Laboratory, University of Pittsburgh, Pittsburgh, Pennsylvania 15213
(Received 6 November 1970)

The reaction $Nb^{93}(d,t)Nb^{92}$ has been studied with a deuteron beam of 17 MeV. Reaction tritons were momentum-analyzed by the Enge split-pole spectrograph and detected by position-sensitive counters as well as nuclear emulsions placed along the focal plane of the spectrograph. The experimental energy resolution was ~8 keV full width at half-maximum. Up to 3 MeV in excitation, approximately 50 states of Nb^{92} have been identified including the 6 previously known low-lying states. Angular distributions for 40 of these triton groups were obtained and l-transfer values for the neutron pickup to the corresponding states in Nb^{92} were assigned by comparison with distorted-wave calculations. A previous classification of the lowest six positive-parity states as belonging to the $(1g_{9/2}^{\pi}2d_{5/2}^{\nu})$ multiplet is confirmed. As there are ambiguities in the assignment of spins to some members of this multiplet on the basis of spectroscopic strengths alone, the electromagnetic-decay properties of the low-lying positive-parity states of Nb^{92} have been studied via the $Nb^{93}(d,t\gamma)Nb^{92}$ reaction. On the basis of the resulting decay scheme, spin assignments are made to the previously identified $(1g_{9/2}^{\pi}2d_{5/2}^{\nu})$ multiplet of states. The 286-, 357-, 480-, and 500-keV states are assigned J^{π} values of 3^+, 5^+, 4^+, and 6^+, respectively.

I. INTRODUCTION

Nuclei with two particles (or two holes) outside a stable core have been treated quite extensively in the literature. The study of such nuclei is of considerable importance for the understanding of the residual nucleon-nucleon interactions. As nuclei in the zirconium region have often been treated successfully on the basis of a fairly simple shell-model structure,[1] a detailed study of Nb^{92} is expected to be very informative.

Previously, Sheline, Watson, and Hamburger (SWH)[2] studied the $Nb^{93}(d, t)Nb^{92}$ reaction at two angles and reported that up to an excitation energy of 2.1 MeV, only six levels of Nb^{92} were seen. Sweet, Bhatt, and Ball[3] studied the analogous $Nb^{93}(p, d)Nb^{92}$ reaction and claimed that up to 3 MeV in excitation the only levels populated were the six low-lying states seen by SWH.[2] These six states were therefore classified as members of the $(1g_{9/2}^{\pi}2d_{5/2}^{\nu})$ sextuplet of states expected on the basis of the simple jj-coupling shell model. In a recent study of another "two-particle nucleus," Sc^{42}, approximately 40 other states were seen up to an excitation energy of 4 MeV in addition to the multiplet of states belonging to the $(f_{7/2})^2$ configuration.[4] Hence the large energy separation suggested for other configurations from $(1g_{9/2}^{\pi}2d_{5/2}^{\nu})$ in Nb^{92} would be very surprising. The purpose of the present high-resolution study of Nb^{92} was threefold: (a) to locate and study the states of Nb^{92} having other configurations, (b) to confirm the identification of the sextuplet of states belonging to the configuration $(1g_{9/2}^{\pi}2d_{5/2}^{\nu})$, and (c) to obtain independent assignments for the spins of some of these states by